

# Synthesis and Material Properties of Syndiotactic Polystyrene/Organophilic Clay Nanocomposites

Mun Ho Kim,<sup>1</sup> Cheon Il Park,<sup>2</sup> Won Mook Choi,<sup>1</sup> Jin Woo Lee,<sup>1</sup> Jae Gon Lim,<sup>3</sup> O Ok Park,<sup>1</sup> Jung Min Kim<sup>4</sup>

<sup>1</sup>Department of Chemical and Biomolecular Engineering, Korea Advanced Institute of Science and Technology, 373-1, Guseong-dong, Yuseong-gu, Daejeon 305-701, Republic of Korea

<sup>2</sup>Chemicals and Polymers Research and Development, LG Chem., Ltd./Research Park, 104-1, Moonji-dong, Yuseong-gu, Daejeon 305-380, Republic of Korea

<sup>3</sup>Polyolefin Development IV Project, Samsung General Chemicals Co. Ltd., San 222-2 Dokgod-Ri, Daesan-Up, Seosan, Chungnam 356-711, Republic of Korea

<sup>4</sup>PVC Plasticizer Team, LG Chem., Ltd./Tech Center, 84, Jang-dong, Yuseong-gu, Daejeon 305-380, Republic of Korea

Received 14 August 2003; accepted 8 December 2003

**ABSTRACT:** Syndiotactic polystyrene (sPS)/organophilic clay nanocomposites were fabricated by direct-melt intercalation method. To overcome the thermal instability of organophilic clay at high-melt processing temperatures of sPS, an organophilic clay modified by alkyl phosphonium was adopted, which is known to be thermally stable. By using the newly synthesized clay, we could fabricate sPS intercalated nanocomposites. The microstructures of nanocomposites were confirmed by X-ray diffraction (XRD) and transmission electron microscopy (TEM). The crystallization rate of nanocomposites investigated by differential scanning cal-

orimetry (DSC) does not increase despite the presence of clay, which may be due to the physical hindrance of organic modifiers in the clay dispersion. Nanocomposites exhibited enhanced mechanical properties such as strength and stiffness relative to the virgin polymer. In addition, thermal stability was confirmed to be improved by thermogravimetric analysis (TGA). © 2004 Wiley Periodicals, Inc. *J Appl Polym Sci* 92: 2144–2150, 2004

**Key words:** syndiotactic polystyrene; clay; alkyl phosphonium; nanocomposite; melt intercalation

## INTRODUCTION

Syndiotactic polystyrene (sPS) is a crystalline polymer with a high-melting point (about 270°C) due to its stereoregularity, whereas atactic polystyrene (aPS) is an amorphous polymer.<sup>1</sup> In addition to the general properties of aPS such as low specific gravity, electrical properties, and hydrolytic stability, sPS possesses not only excellent heat and chemical resistance but also dimensional stability.<sup>2</sup> Therefore, sPS is thought to be one of the most promising candidates for a new engineering thermoplastic.

The polymer–clay nanocomposite has received considerable attention because of its various advantages over the conventional polymer composites. With even a small amount of clay, nanocomposites show enhanced mechanical and thermal properties, low gas permeability, chemical resistance, and flame retardancy because of nanoscale effects and a large interface area.<sup>3–7</sup>

Polymer-layered silicate nanocomposites were prepared in three ways: *in situ* intercalation, solution intercalation, and melt intercalation. Recently, the third method has attracted extensive interest because this method is environmentally friendly because of the absence of organic solvents. Furthermore, this method is compatible with current polymer processing techniques such as injection molding and extrusion. Through this method, it is possible to fabricate the nanocomposite of polymers which were previously not suitable for *in situ* and solution intercalation.<sup>8,9</sup>

sPS/clay nanocomposites were mainly prepared by solution intercalation method.<sup>10–12</sup> It was impossible to fabricate the sPS/clay nanocomposites by direct-melt intercalation method. Generally, silicate should be modified with alkyl ammonium for the polymer to penetrate easily into the silicate layer because alkyl ammonium makes the hydrophilic silicate surface organophilic. However, the interaction between alkyl ammonium and the silicate layer is not thermally stable enough to resist the high-melt processing temperatures of sPS (about 280°C), which makes the melt intercalation of sPS into the clay gallery difficult. That is to say, fabrication of the nanocomposites by direct-melt intercalation of sPS into organophilic clay is problematic because of the thermal instability of the

Correspondence to: O O. Park (ookpark@kaist.ac.kr).

organic modifier (alkyl ammonium) treated on the inner surface layer of the clay.<sup>13,14</sup> To solve this problem, an indirect approach was used to fabricate sPS/organophilic clay nanocomposites: melt intercalation of amorphous styrenic polymers into organophilic clay followed by blending with sPS.<sup>15</sup> It has been thought that the use of amorphous styrenic polymer is inevitable for the fabrication of sPS nanocomposites.

In this article, we attempted to fabricate the nanocomposite of an sPS/clay system by direct-melt intercalation without using amorphous styrenic polymers. If we do not use the amorphous styrenic polymers, the fabrication process will be simpler and deterioration in mechanical properties due to the introduction of the amorphous styrenic polymers in crystalline sPS matrix will disappear. To do this, the thermally stable organophilic clay is needed. Therefore, we decided to fabricate and use the organophilic clay which is modified by alkyl phosphonium instead of the commonly used alkyl ammonium. It is well known that alkyl phosphonium treated clay is more thermally stable than alkyl ammonium treated clay.<sup>16</sup>

On the basis of the above fabrication method, we first investigated the thermal stability of organophilic clay modified by alkyl phosphonium to prove the feasibility of the above fabrication method. In addition, the microstructure of the fabricated sPS nanocomposites is examined by X-ray diffraction (XRD) and a transmission electron microscope (TEM). Then, the crystallization behavior of nanocomposites was investigated. Finally, the mechanical and thermal properties of sPS nanocomposites are considered.

## EXPERIMENTAL

### Materials

The sPS used in this study had a weight-average molecular weight ( $M_w$ ) of 256,000, was supplied by Samsung General Chemical Co., and was used as received. Sodium-montmorillonite ( $\text{Na}^+$ -MMT) was supplied by the Southern Clay Co., and the cation exchange capacity (CEC) of this clay was 95 meq/100 g. Hexadecyltributyl phosphonium bromide, a cationic surfactant, was purchased from Aldrich.

### Preparation of organophilic clay

Organophilic clay was synthesized by a cation exchange reaction between the clay particles and alkyl phosphonium salt. The modification of montmorillonite was carried out as follows. Sodium-montmorillonite (15 g; 95 meq/100 g) was dispersed into 1500 mL distilled water (70°C) by using a homogenizer. Hexadecyltributyl phosphonium bromide (7.96 g) (mont-

morillonite/phosphonium salt = 1/1.1 in CEC) was dissolved into 500 mL distilled water (70°C). It was poured into montmorillonite–water solution and stirred vigorously for 30 min by using a homogenizer to yield the white precipitate. Then, the white precipitate was filtered and washed three times with 2000 mL of distilled water (70°C). The product was kept in a vacuum oven at 80°C for 24 h and ground by using a mortar and pestle. Particles with a size less than 50  $\mu\text{m}$  were collected.

### Preparation of the nanocomposite

A preweighed amount of organophilic clay and sPS powder were mixed together at room temperature and then melt mixed in a Haake Rheomixer 600 at 280°C for 6 min with 50 rpm rotor speed. After completion of the mixing, the mixed composites were ejected from the mixing chamber and cooled at room temperature.

### Measurements

XRD spectra were obtained by using a Rigaku X-ray generator ( $\text{CuK}\alpha$  radiation with  $\lambda = 1.5406 \text{ \AA}$ ) with a  $2\theta$  scan range of 0 to 10° at room temperature. The specimens of the nanocomposite for XRD measurement were obtained in sheet form by using a hydraulic press at 280°C. The dispersion state and layered structure of the clay were observed by using a Jeol JEM-2000EX TEM. The specimens were cut into ultrathin slices by using a Reichert–Jung Ultracut Microtome at room temperature without any staining process.

Crystallization behavior of nanocomposites was investigated by using differential scanning calorimetry (DSC; DuPont TA 2010). The samples were heated to 310°C under a nitrogen atmosphere and held in the melt state for 5 min to eliminate the influence of thermal history. Then, these samples were cooled at different cooling rates of 6, 10, 14, and 20°C/min. The obtained thermograms were analyzed in estimating the crystallization kinetics.

Tensile properties and flexural modulus were measured as the mechanical properties of the nanocomposites. Tensile tests were performed by using a universal tensile machine (Instron UTM) according to the test method of ASTM D 1708. The crosshead speed was 1 mm/min. The flexural modulus was also obtained by using UTM according to the test method of ASTM D 790. The crosshead speed was 5 mm/min.

TA Instruments thermogravimetric analyses (TGA) were performed as the thermal properties of the nanocomposite. Samples were heated to 600°C at a heating rate of 10°C/min under an air atmosphere.

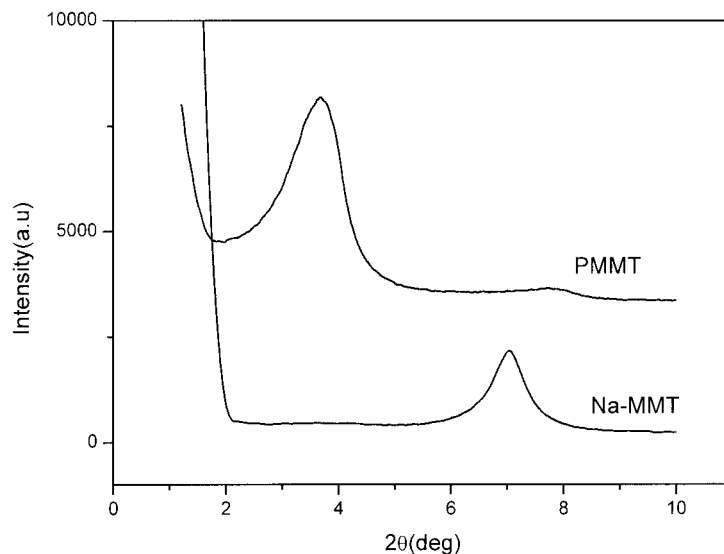


Figure 1 XRD pattern of organophilic clay.

## RESULTS AND DISCUSSION

### Thermal characterization of organophilic clay

The XRD patterns of the clay are shown in Figure 1. The XRD pattern of sodium montmorillonite shows basal reflections characteristic of  $2\theta = 7.0^\circ$ . Organophilic clay treated by hexadecyltributyl phosphonium (PMMT) has the (001) peak at  $2\theta = 3.7^\circ$ . By Bragg's rule, the  $d$ -space of clay increases from 1.26 to 2.40 nm. This result indicates that the hexadecyltributyl phosphonium is indeed intercalated into the layers of clay and the hydrophilic silicate surface changes into an organophilic surface. Thus, the sPS chains can be more easily intercalated into the space of the silicate layers.

For the fabrication of sPS nanocomposites via melt intercalation, organophilic clay should have thermal stability at high-melt processing temperatures of  $280^\circ\text{C}$ . We investigated the thermal stability of PMMT in comparison with the commonly used organophilic clays modified by alkyl ammonium (Cloisite® 15A and 10A, Southern Clay Co.). The inner layer surfaces of each organoclay are treated by dimethyl dihydrogenated tallow ammonium (15A) and dimethyl benzyl hydrogenated tallow ammonium (10A). By TGA, as shown in Figure 2, it was shown that about 70 wt % of the alkyl ammonium material was degraded at  $280^\circ\text{C}$ , the melting processing temperature of sPS. This high amount of weight loss of organic material brings

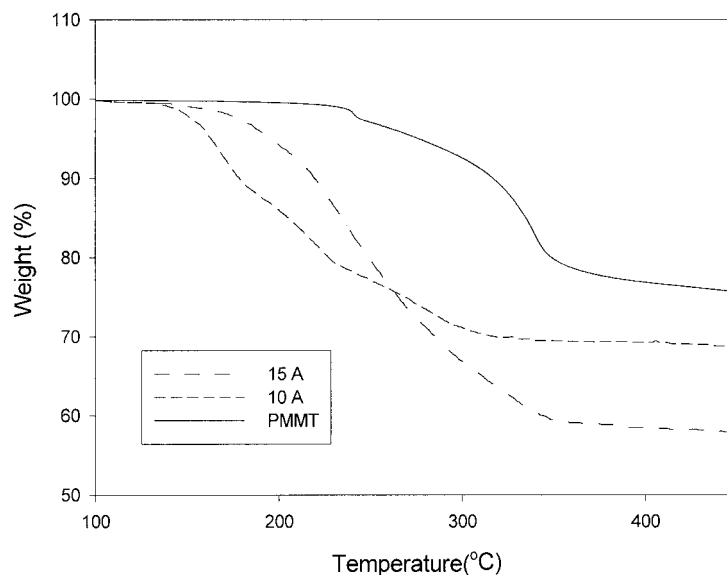


Figure 2 TGA curves of organophilic clays.

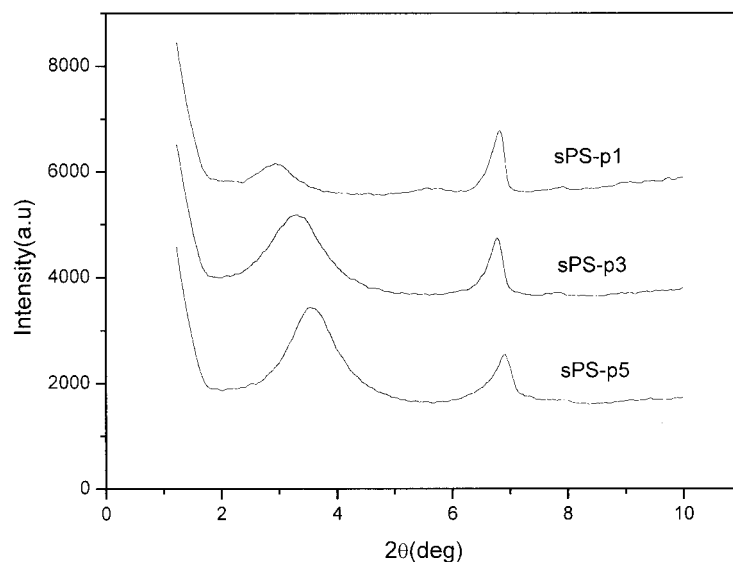


Figure 3 XRD patterns of sPS/PMMT nanocomposites.

about the decrease of interlayer spacing and deteriorates the compatibility of silicates with polymer, which hinders the intercalation of sPS into the clay gallery. In the case of PMMT, however, most of the organic material was not degraded at 280°C. This result indicates that PMMT is more thermally stable than the commonly used organophilic clays. Thus, it is expected that sPS/PMMT nanocomposites can be obtained by direct-melt intercalation.

#### Microstructure of sPS nanocomposites

sPS nanocomposites were obtained by direct-melt intercalation. The organophilic clay contents were 1, 3, and 5 wt %. To investigate the microstructure of sPS nanocomposites, XRD and TEM experiments are required. The *d*-space of clay can be estimated by XRD, and the dispersion of clay can be shown by TEM.

The XRD patterns of fabricated sPS nanocomposites are shown in Figure 3. The peaks around  $2\theta = 6.7^\circ$ , known to be the  $\alpha$ -form crystal peak of sPS itself,<sup>17</sup> are also seen in the figure. By Bragg's rule, we could know that the *d*-space of clay in sPS nanocomposites in-

creased from 0.2 to 0.6 nm relative to the original modified clay. This result indicates that sPS intercalated nanocomposites are formed. The XRD data are summarized in Table I.

The microstructures of sPS nanocomposite (clay content of 3 wt %) observed by TEM are shown in Figure 4. Individual layers of clay are visible as a region of narrow dark bands. The layered structure of clay intercalated by polymer is obvious. This result is consistent with the XRD results.

As shown in XRD and TEM results, we could fabricate sPS intercalated nanocomposites by direct-melt intercalation method by using thermally stable organophilic clay. As compared with the existing stepwise melt intercalation method,<sup>15</sup> this method is much simpler and therefore a more economical process.

TABLE I  
The Compositions of sPS Nanocomposites and Their *d*-spaces

Abbreviation	sPS (wt %)	Organophilic clay, PMMT (wt %)	<i>d</i> -space (nm)
sPS	100	0	—
sPS-p1	99	1	3.04
sPS-p3	97	3	2.68
sPS-p5	95	5	2.52
PMMT	0	100	2.40

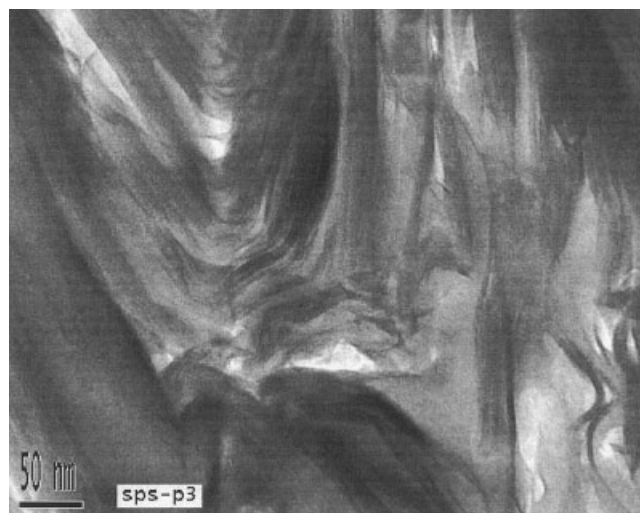


Figure 4 TEM image of sPS/PMMT nanocomposite.

**TABLE II**  
Nonisothermal Crystallization Data of sPS Nanocomposites

Sample	Cooling rate (°C/min)	$T_c$ (°C)	$\Delta H_c$ (J/g)	$t_{1/2}$ (min)
sPS	6	238.5	24.34	1.273
	10	235.3	24.33	0.791
	14	232.2	23.84	0.694
	20	230.3	24.18	0.518
sPS-p1	6	238.6	23.88	1.201
	10	234.5	24.35	0.921
	14	231.3	23.57	0.728
	20	229.2	23.93	0.514
sPS-p3	6	237.7	23.93	1.272
	10	235.3	23.74	0.855
	14	231.4	23.49	0.702
	20	228.6	22.99	0.523
sPS-p5	6	234.0	22.49	1.511
	10	234.6	23.40	0.845
	14	230.1	21.76	0.672
	20	226.8	22.40	0.574

### Crystallization behavior of sPS nanocomposites

It is important to investigate the crystallization behavior that occurred during processing as injection molding because sPS is a semicrystalline polymer. At first, a nonisothermal crystalline study was performed for sPS nanocomposites. It seems desirable to study crystallization behaviors under nonisothermal conditions because the isothermal crystallization condition is rarely achievable in practical processing. There have been many suggestions to make a material parameter for directly comparing crystallization rates. Among them, we adopted the crystallization rate parameter (CRP) proposed by Zhang et al.<sup>18</sup> From the nonisothermal crystallization thermograms, the width of the crystallization exothermic peak at half-height divided by the cooling rate yields the isothermal crystallization half-time,  $t_{1/2}$ , necessary for performing one-half a transition process at a given crystallization temperature. Polymeric material having a slower crystallization rate has a larger  $t_{1/2}$ . The CRP is determined by the slope in cooling rate versus  $1/t_{1/2}$  plot and corresponds to the crystallization rate of the system.

The crystallization temperature ( $T_c$ ), heat of crystallization ( $\Delta H_c$ ), and half-time of crystallization ( $t_{1/2}$ ) obtained from thermograms were summarized in Table II.  $T_c$  decreased with the increasing cooling rate, which commonly occurs in polymeric systems due to the difference in time scale between the transformation of polymer chains to crystalline and the cooling rate.  $\Delta H_c$  values of sPS nanocomposites are lower than those of the sPS matrix. This indicates that the crystalline portion was reduced. It seems that the presence of clay hinders the transportation of polymer chains and ultimately crystal growth.

When the reciprocal of  $t_{1/2}$  was plotted against the cooling rate, the linear plots were obtained for all

samples, as reported previously by Zhang et al. The slopes of these plots (i.e., CRP) were obtained by linear regression. These CRP values were plotted against the clay content in Figure 5. From this figure, we could observe that the overall crystallization rate hardly changes with clay content. That is, the nucleation effect of clay is not found in this system. This result is consistent with the tendency that the  $T_c$  value of sPS nanocomposites is slightly lower than that of the pure sPS, as shown in Table II. In this system, the nucleation effect of clay is not high because the clay layers are not exfoliated. Moreover, bulky hexadecyltributyl phosphonium molecules of PMMT are thought to interfere with the nucleation mechanism by physical hindrance within the sPS matrix.<sup>10</sup> Therefore, the overall crystallization rate does not increase despite the addition of clay.

### Mechanical properties of sPS nanocomposites

Tensile strength, tensile modulus, and flexural modulus were measured as mechanical properties. Figure 6 shows the mechanical properties of sPS nanocomposites as a function of the clay loading. As the content of clay increases, the tensile properties of nanocomposites increase gradually due to the nanoscaled hybrid of polymer and clay. Flexural modulus also increases with the increase in clay contents.

In stepwise melt intercalation systems, a large amount of clay was added for mechanical properties enhancement because amorphous styrenic polymers affect the mechanical properties negatively in crystalline sPS matrix.<sup>15</sup> In the present system, however, sPS nanocomposites show enhanced mechanical properties at the low content of clay.

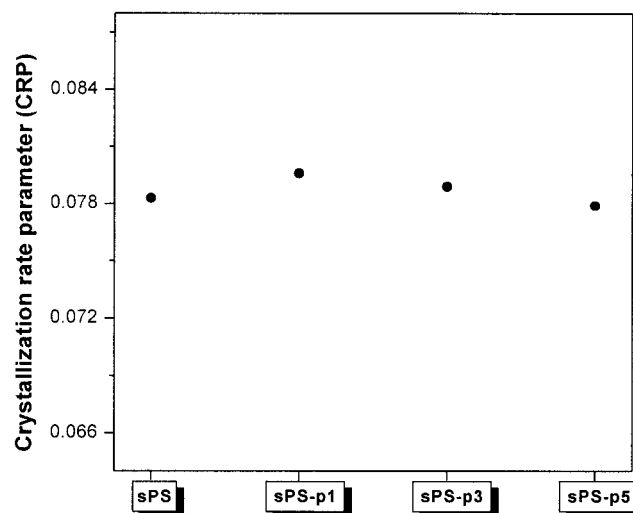


**Figure 5** Crystallization rate parameter (CRP) of sPS nanocomposites.

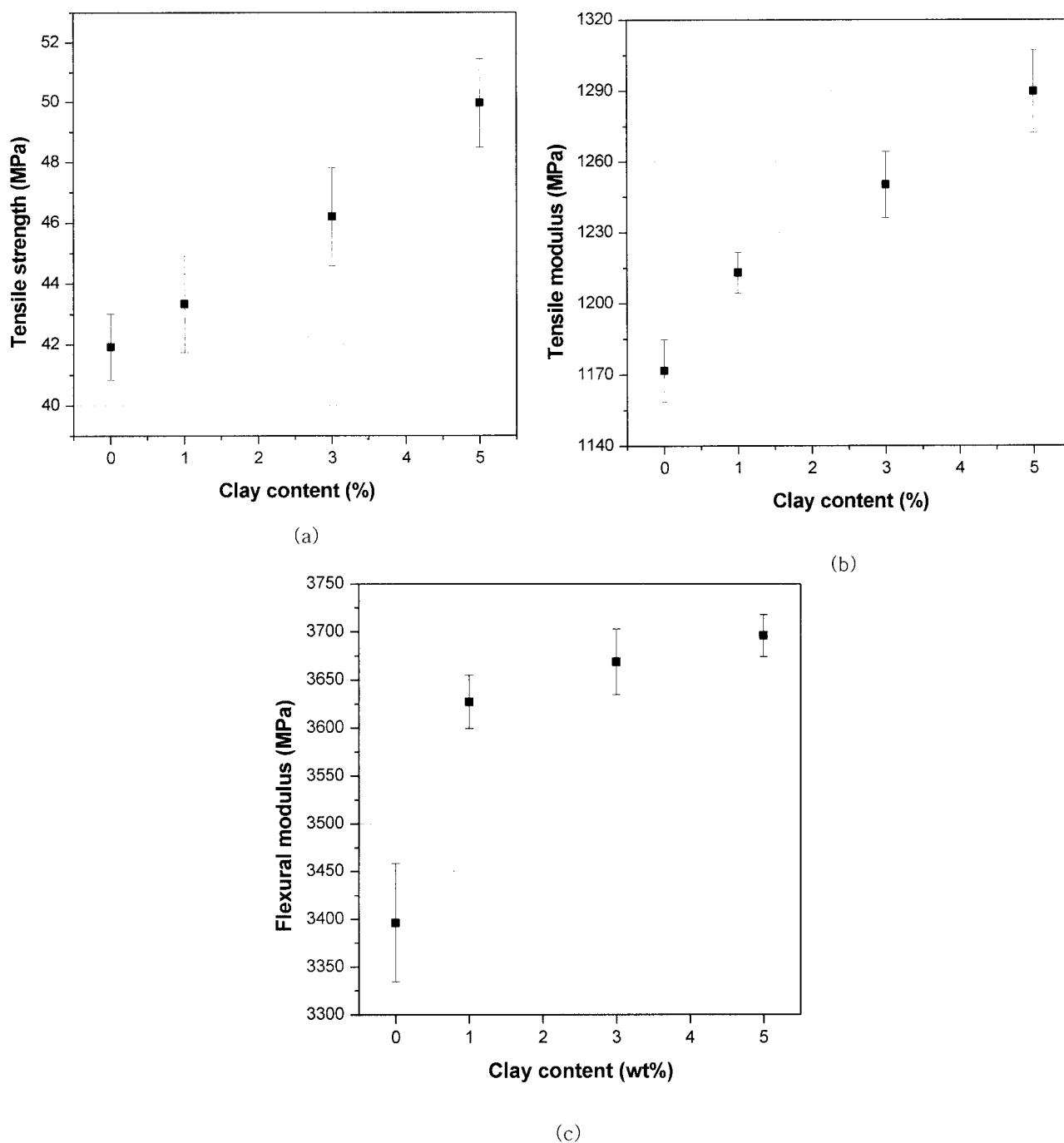


Figure 6 Mechanical properties of sPS nanocomposites: (a) tensile strength; (b) tensile modulus; (c) flexural modulus.

### Thermal properties of sPS nanocomposites

Figure 7 shows TGA thermograms of the virgin sPS and sPS nanocomposites. As the content of clay increases, TGA curves of sPS nanocomposites show delayed decomposition relative to the virgin sPS, and the decomposition onset temperature of sPS nanocomposites increases with clay contents. Thus, it is clear that sPS nanocomposites are more thermally stable than the virgin sPS. This increased thermal stability results from hindered out-diffusion of the volatile decompo-

sition products. We saw a multilayered silicate structure in sPS nanocomposites by means of TEM. It is expected that this multilayer silicate array serves as an excellent insulator and mass transport barrier, thus slowing down the out-diffusion of volatile decomposition products.<sup>19,20</sup> Additionally, it seems that the organic modifier containing a phosphonium plays some role in increased thermal stability. It is well known that phosphorous compounds are effective flame retardants.

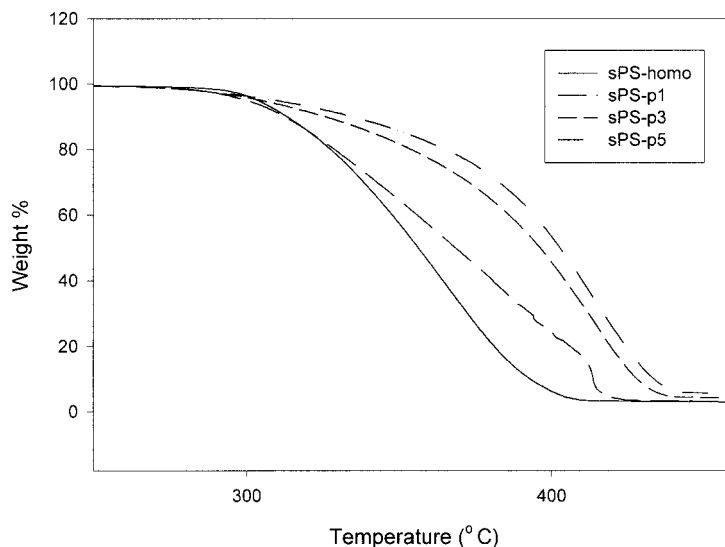


Figure 7 TGA thermograms of sPS nanocomposites.

### CONCLUSION

The fabrication of sPS nanocomposites was conducted by the direct-melt intercalation method. To avoid the thermal instability problem of organophilic clay, we fabricated and used the organophilic clay modified by alkyl phosphonium instead of the more commonly used organophilic clay modified by alkyl ammonium. The fabricated organophilic clay (PMMT) was thermally stable enough to resist high-melt processing temperatures of sPS. By using PMMT, we could obtain sPS nanocomposites by melt intercalation without using amorphous styrenic polymers. sPS nanocomposites showed enhanced materials properties. We believe that the present work is useful for the fabrication of nanocomposites of other polymers with high-processing temperature.

The authors are very grateful for the financial support provided by Samsung General Chemical Ltd. and the Center for Advanced Functional Polymers through KOSEF. In addition, this work was also partially supported by the Brain Korea 21 project of the Ministry of Education (MOE) of Korea.

### References

- Ishihara, N.; Seimiya, T.; Kuramoto, M.; Uoi, M. *Macromolecules* 1986, 19, 2464.
- Malanga, M. *Adv Mater* 2000, 12, 1869.
- Giannelis, E. P. *Adv Mater* 1996, 8, 29.
- LeBaron, P. C.; Wang, Z.; Pinnavaia, T. *Appl Clay Sci* 1999, 15, 11.
- Giannelis, E. P.; Krishnamoorti, R.; Manias, E. *Adv Polym Sci* 1999, 138, 107.
- Carrado, K. A. *Appl Clay Sci* 2000, 17, 1.
- Alexandre, M.; Dubois, P. *Mat Sci Eng R* 2000, 28, 1.
- Kawasumi, M.; Hasegawa, N.; Kato, M.; Usuki, A.; Okata, A. *Macromolecules* 1997, 30, 6333.
- Giannelis, E. P. *Appl Organomet Chem* 1998, 12, 675.
- Tseng, C. R.; Lee, H. Y.; Chang, F. C. *J Polym Sci, Part B: Polym Phys* 2001, 39, 2097.
- Tseng, C. R.; Wu, J. Y.; Lee, H. Y.; Chang, F. C. *Polymer* 2001, 42, 10063.
- Wu, T. M.; Hsu, S. F.; Wu, J. Y. *J Polym Sci, Part B: Polym Phys* 2002, 40, 736.
- Lee, J. W.; Lim, Y. T.; Park, O. O. *Polym Bull* 2000, 45, 191.
- Gilman, J. W.; Jackson, C. L.; Morgan, A. B.; Harris, R., Jr. *Chem Mater* 2000, 12, 1866.
- Park, C. I.; Park, O. O.; Lim, J. G.; Kim, H. J. *Polymer* 2001, 42, 7465.
- Takekoshi, T.; Khouri, F. F.; Campbell, J. R.; Jordan, T. C.; Dai, K. H. *U.S. Pat. 5,707,439*, 1998.
- Lin, R. H.; Woo, E. M. *Polymer* 2000, 41, 121.
- Zhang, R.; Zheng, H.; Lou, X.; Ma, D. *J Appl Polym Sci* 1994, 51, 51.
- Doh, J. D.; Cho, I. *Polym Bull* 1998, 41, 511.
- Dietsche, F.; Mulhaupt, R. *Polym Bull* 1999, 43, 395.